

Fate of the conformal fixed point with twelve massless fermions and SU(3) gauge group

Zoltan Fodor,¹ Kieran Holland,² Julius Kuti,³ Santanu Mondal,⁴ Daniel Nogradi,⁴ and Chik Him Wong⁵

¹*University of Wuppertal, Department of Physics, Wuppertal D-42097, Germany, and Juelich Supercomputing Center, Forschungszentrum Juelich, Juelich D-52425, Germany*

²*University of the Pacific, 3601 Pacific Ave, Stockton, California 95211, USA*

³*University of California, San Diego, 9500 Gilman Drive, La Jolla, California 92093, USA*

⁴*Eötvös University, Institute for Theoretical Physics,*

MTA-ELTE Lendulet Lattice Gauge Theory Research Group, Budapest 1117, Hungary

⁵*University of Wuppertal, Department of Physics, Wuppertal D-42097, Germany*

(Received 21 July 2016; published 9 November 2016)

We report new results on the conformal properties of an important strongly coupled gauge theory, a building block of composite Higgs models beyond the Standard Model. With twelve massless fermions in the fundamental representation of the SU(3) color gauge group, an infrared fixed point (IRFP) of the β -function was recently reported in the theory [A. Cheng, A. Hasenfratz, Y. Liu, G. Petropoulos, and D. Schaich, J. High Energy Phys. 05 (2014) 137] with uncertainty in the location of the critical gauge coupling inside the narrow $[6.0 < g_*^2 < 6.4]$ interval and widely accepted since as the strongest evidence for a conformal fixed point and scale invariance in the theory with model-building implications. Using the exact same renormalization scheme as the previous study, we show that no fixed point of the β -function exists in the reported interval. Our findings eliminate the only seemingly credible evidence for conformal fixed point and scale invariance in the $N_f = 12$ model whose infrared properties remain unresolved. The implications of the recently completed 5-loop QCD β -function for arbitrary flavor number are discussed with respect to our work.

DOI: [10.1103/PhysRevD.94.091501](https://doi.org/10.1103/PhysRevD.94.091501)

I. INTRODUCTION AND MOTIVATION

Investigations of strongly coupled gauge theories with massless fermions in the fundamental or two-index symmetric (sextet) representation of the SU(3) color gauge group serve considerable theoretical interest with added relevance as important building blocks of composite Higgs theories beyond the Standard Model (BSM). Two complementary aspects of the composite Higgs paradigm are investigated in this large class of theories: (1) a near-conformal and unexpectedly light scalar particle, perhaps dilatonlike with mass at the electroweak scale or (2) a parametrically light pseudo Nambu-Goldstone boson (PNGB) combined with partial compositeness for fermion mass generation to avoid the flavor problem. Both paradigms are based on strongly coupled gauge dynamics to address important aspects of conformal and chiral symmetries and their symmetry breaking patterns in BSM theories. The precise determination of near-conformal or conformal behavior of SU(3) gauge theory with twelve flavors is relevant for both paradigms.

(1) *Light scalar, perhaps dilatonlike?* Near-conformal strong dynamics with spontaneous chiral symmetry breaking (χ SB) is focused on its emergent light scalar with 0^{++} quantum numbers of the σ -meson, perhaps with dilatonlike properties. With early results reviewed in [1], this paradigm is very different from scaled up quantum chromodynamics (QCD) which was the prototype of old Higgs-less

technicolor. Comparing near-conformal models, with details explained in Fig. 1, a light composite scalar of the massless SU(2) flavor doublet in the sextet fermion representation of SU(3) color was reported in [1,2] whereas the $N_f = 8$ light scalar with fermions in the fundamental representation was discovered in [3] and confirmed recently [4]. The sextet model β -function, with the minimal flavor doublet required for the composite Higgs mechanism, indicates the closest position to the lower edge of the conformal window (CW) among recently investigated SU(3) gauge theories, exhibiting the lightest scalar accordingly. The β -function of the sextet theory with three massless flavors has a weakly coupled conformal fixed point close to the upper end of the CW [5] with apparent crossing into the CW between two and three flavors. In contrast, uncertainties in crossing into the CW with fermions in the fundamental representation appear to extend into the wider $N_f = 8$ –12 flavor range. For example, it is not known if for more than eight flavors the theory gets very close to the CW with a much lighter scalar mass than at $N_f = 8$. Based on the findings of [6] and a similar zero in the β -function reported earlier [7,8], the $N_f = 12$ model has been investigated as a composite Higgs model built on a conformal fixed point inside the CW [9]. The importance of the question warrants independent determination.

(2) *PNGB with partial compositeness?* Challenges for the near-conformal light scalar paradigm to generate fermion

masses and Yukawa couplings motivates the alternate PNGB scenario with a massless scalar boson emerging from vacuum misalignment of χSB as reviewed recently [14]. Model studies with a parametrically light Higgs based on $N_f = n_f + \nu_f$ fermion flavors in the fundamental representation of the SU(3) color gauge group could address the hierarchy problem and fermion mass generation with partial compositeness, if N_f is large enough to bring the theory inside the CW before mass deformations of conformal symmetries are turned on [14–16]. For the simple choice $n_f = 4$, the global flavor symmetry $SU(4) \times SU(4)$ is broken to the diagonal SU(4) flavor group and a Higgs-like scalar state is identified in the PNGB set via χSB . The custodial SO(4) symmetry of the Standard Model remains protected [15,16] while a large enough ν_f is required to bring the theory close to a strongly coupled IRFP with expectations of large baryon anomalous dimensions as the key ingredients of partial compositeness. The $N_f = 12$ choice with $n_f = 4$ and $\nu_f = 8$ for this PNGB paradigm is discussed in [9] building on the conformal fixed point of twelve flavors, warranting again independent confirmation.

II. LATTICE IMPLEMENTATION OF THE STEP β -FUNCTION

The gradient flow based diffusion of the gauge fields of lattice configurations from Hybrid Monte Carlo (HMC) simulations became the method of choice for studying renormalization effects with great accuracy [17–23]. In particular, we adapted the method and introduced the scale-dependent renormalized gauge coupling $g^2(L)$ where the scale is set by the linear size L of the finite volume [10,24]. This implementation is based on the gauge invariant trace of the non-Abelian quadratic field strength, $E(t) = -\frac{1}{2} \text{Tr} F_{\mu\nu} F_{\mu\nu}(t)$, renormalized as a composite operator at gradient flow time t on the gauge configurations and measured from the discretized lattice implementation, as in [20]. Following [10,24], we define the one-parameter family of renormalized nonperturbative gauge couplings for strongly coupled gauge theories built on the SU(N) color group with N_f massless dynamical fermions,

$$g_c^2(t(L)) = \frac{128\pi^2 \langle t^2 E(t) \rangle}{3(N^2 - 1)(1 + \delta(c))}, \quad (1)$$

where the volume-dependent gradient flow time $t(L)$ is set by the constant $c = \sqrt{8t}/L$ from the one-parameter family of renormalization schemes, with $c = 0.2$ chosen in this work. The factor

$$\delta(c) = -\frac{c^4 \pi^2}{3} + \vartheta^4(e^{-1/c^2}) - 1 \quad (2)$$

in Eq. (1) is chosen to match $g_c^2(t(L))$ to the conventional coupling $g_{\text{MS}}^2(t(L))$ in leading order of perturbation theory for any choice of c and with periodic boundary conditions

for the gauge fields in all four directions. The origin of the third Jacobi elliptic function ϑ in Eq. (2) was explained in [10] including the treatment of zero modes from periodic gauge fields in finite volumes [25–29].

A scale-dependent renormalized gauge coupling $g^2(L)$ was introduced earlier to probe the step β -function, defined as $(g^2(sL) - g^2(L))/\log(s^2)$ for some preset finite scale change s in the linear physical size L of the four-dimensional volume in the continuum limit of lattice discretization [30,31]. The gauge coupling $g^2(L)$ for the determination of the step β -function is identified in our case with the definition in Eq. (1) as we drop the preset label c in the notation and $t(L)$ is simply replaced by L . The renormalization scheme with the preset choice $c = 0.2$ and the preset scale factor $s = 2$ in our work is identical to the one of the previous study [6] including the boundary conditions on gauge fields and fermion fields. In the continuum limit, the monotonic function $g^2(L)$ implies in any of the volume-dependent schemes that a selected value of the renormalized gauge coupling sets the physical size L measured in some particular dimensionful physical unit. Fixed physical size L on the lattice is equivalent to holding $g^2(L)$ fixed at some selected value as the lattice spacing a is varied and the fixed physical length L is held by the variation of the dimensionless linear scale L/a as the bare lattice coupling is tuned without changing the selected fixed value of the renormalized gauge coupling. The continuum limit at fixed $g^2(L)$ is obtained by $a^2/L^2 \rightarrow 0$ extrapolation of the residual cutoff dependence in the step β -function at the target gauge coupling.

In the convention we use, asymptotic freedom in the UV regime corresponds to a positive step β -function given by the perturbative loop expansion for small values of the renormalized coupling. In the infinitesimal derivative limit $s \rightarrow 1$ the step β -function turns into the conventional one. If the conventional β -function of the theory possesses a fixed point, the step β -function will have a zero at the same critical gauge coupling g_*^2 as well. The scale-dependence of the gauge coupling $g^2(L)$ can be determined from repeated application of the step β -function starting at some scale L_0 set by the initial gauge coupling $g^2(L_0)$ we choose.

III. BSM MODELS CLOSE TO THE CONFORMAL WINDOW

The effect of near-conformal behavior on the light scalar mass is shown in Fig. 1, if the size of the nonperturbative β -function is used at strong coupling as an indicator for the approach to the CW in the fundamental and sextet representations of massless fermions. The mass of the light σ -like 0^{++} scalar particle, as a composite Higgs candidate when coupled to the electroweak sector, is displayed in units of the Goldstone decay constant F in the massless fermion limit of χSB as determined from spectroscopy in each model. The striking trend of decreasing scalar mass is

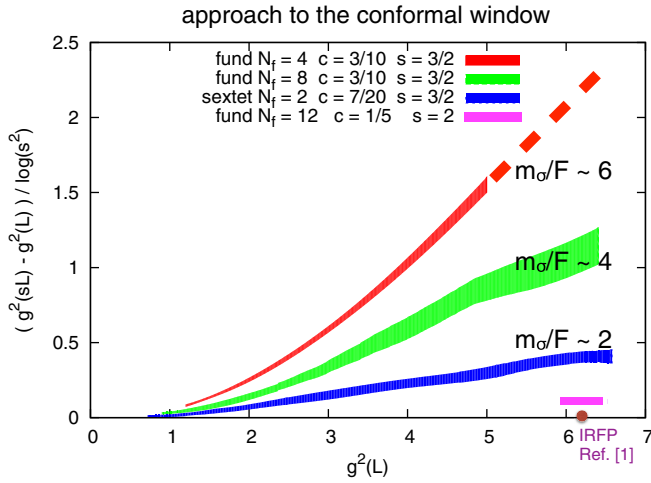


FIG. 1. The step β -functions of strongly coupled gauge theories in two different fermion representations of the SU(3) gauge group are color coded. The $N_f = 4$ β -function is from [10] (dashed line segment extrapolated) with the m_σ/F ratio taken from QCD, the $N_f = 8$ β -function is from [11] with the m_σ/F ratio from [3,4], and the sextet β -function is from [12] with the m_σ/F ratio taken from [13]. The magenta IRFP of $N_f = 12$ is from [6] and the magenta line of our new nonvanishing $N_f = 12$ β -function is also shown in the ~ 0.1 range.

well established as the CW is approached. In BSM applications $F = 250 \text{ GeV}$ sets the scale in physical units [1]. The sextet model has the smallest nonzero β -function relative to the other theories in the fundamental representation, together with the lightest scalar. The possibility of the $N_f = 12$ model being even closer to the CW with an even lighter scalar is open, if the model is near-conformal without IRFP. Our goal is an independent determination of the fate of the $N_f = 12$ IRFP reported earlier [6].

IV. $N_f = 12$ SIMULATIONS WITH TARGETED RUN SETS

The algorithmic details of our new $N_f = 12$ simulations are similar to [10,11]. Periodic boundary conditions already

defined on the gauge fields, the fermion fields are chosen to be antiperiodic in all four directions. We utilize the staggered fermion action with massless fermions and four steps of stout smearing with stout parameter $\varrho = 0.12$ on the gauge links [17]. The gauge action is the tree-level improved Symanzik action [32,33]. The evolution along a trajectory of the Hybrid Monte Carlo algorithm [34] is implemented with multiple time scales [35] and Omelyan integrator [36]. For integration along the gradient flow we use the tree-level improved Symanzik action based discretization scheme. The observable $E(t)$ is discretized as in [20].

The final 28 runs of Table I ranged in length between 5000 and 20,000 time units of molecular dynamics. The statistical analysis of the renormalized gauge coupling of each run followed [37] and used similar software. Autocorrelation times were measured for each run in two independent ways, using estimates from the autocorrelation function of each run, and from jackknifed blocking procedure. Errors on the renormalized couplings were consistent from the two procedures and the one from autocorrelation functions is listed in Table I. Each run went through thermalization and these segments were not included in the analysis. For detection of residual thermalization effects the replica method of [37] was used in the analysis. All 28 runs passed Q value tests when mean values and statistical errors of the replica segments were compared for thermal and other variations.

We targeted the step β -function at three preselected values of the renormalized gauge coupling to cover the interval where the IRFP was reported [6]. In Table I results are shown for gauge ensembles from the three target groups A, B, C of the final run sets. The 28 runs were grouped into 14 steps of pairs where the lower L/a value was precisely tuned to the target value of the renormalized gauge coupling. The higher L/a volume at the doubled physical size determined the step β -function at finite lattice spacing. The first group with 4 steps is target A at $g^2(L) = 5.979(2)$ with $L/a = 16 \rightarrow 32, 18 \rightarrow 36, 20 \rightarrow 40, 24 \rightarrow 48$. Both target B at $g^2(L) = 6.185(2)$

TABLE I. The final 28 runs are tabulated with 14 tuned runs and 14 paired steps.

L/a	Target A		Target B		Target C	
	$6/g_0^2$	g^2	$6/g_0^2$	g^2	$6/g_0^2$	g^2
16	3.1519	5.9801(29)	3.0830	6.1786(39)	3.0110	6.3930(30)
32	3.1519	5.9952(79)	3.0830	6.1597(64)	3.0110	6.3233(74)
18	3.1510	5.9767(40)	3.0785	6.1871(37)	3.0055	6.3909(51)
36	3.1510	6.0101(71)	3.0785	6.1840(81)	3.0055	6.3446(64)
20	3.1499	5.9828(64)	3.0704	6.1922(64)	2.9896	6.3942(59)
40	3.1499	6.0419(73)	3.0704	6.2137(67)	2.9896	6.4000(67)
24	3.1480	5.9784(68)	3.0680	6.1861(55)	2.9800	6.3976(60)
48	3.1480	6.0758(84)	3.0680	6.2497(109)	2.9800	6.4404(122)
28			3.0698	6.1839(58)	2.9819	6.3900(37)
56			3.0698	6.2792(142)	2.9819	6.4610(124)

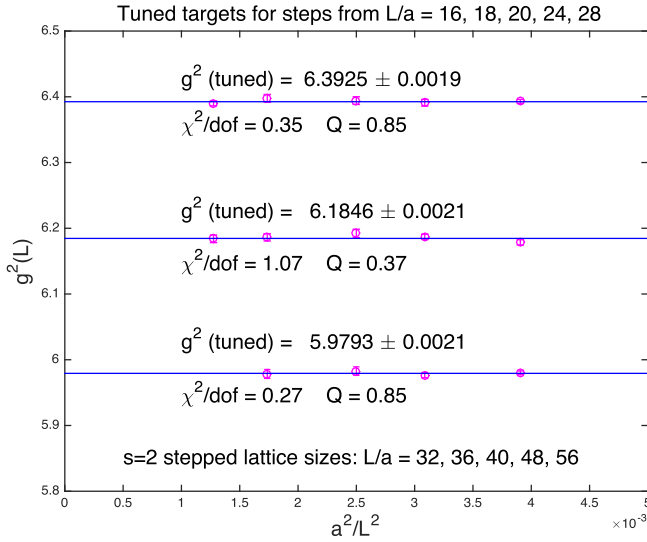


FIG. 2. The statistical significance of precise tuning to three targeted gauge couplings is shown by fitting a constant to each g^2 at the lower L/a values of the steps.

and target C at $g^2(L) = 6.393(2)$ have an added fifth step of $L/a = 28 \rightarrow 56$ for more robust continuum extrapolation. Precise tuning for g_0^2 of the 14 steps of the three targets eliminated the largest systematic uncertainty in the step β -function from model-dependent interpolation in the bare gauge coupling. Figure 2 shows the remarkable accuracy of tuning for the three targets at better than per mille accuracy level, like for the entries of Table I.

V. CONTINUUM EXTRAPOLATION OF THE STEP β -FUNCTION

Cutoff effects have to be removed from the step β -functions at finite lattice spacing. The leading cutoff effects are a^2/L^2 corrections in each $L/a \rightarrow 2L/a$ pair for the step β -function at the targeted renormalized couplings. Linear fits to the lattice step functions in a^2/L^2 allows continuum extrapolation to the $a^2/L^2 \rightarrow 0$ limit, as shown in Fig. 3. For all three targets linear four-point fits of the step functions were used with consistently good χ^2 results. The final results of our continuum step β -function are shown in Fig. 4 with overwhelming statistical evidence against the IRFP of [6] in the targeted interval. Leaving open the existence of the IRFP in [6], a new study of the β -function appeared recently in a different renormalization scheme of the model and without our targeted goal [38].

VI. NEW DEVELOPMENTS AND CONCLUSIONS

Originally the zero of the β -function for twelve flavors was reported at a somewhat lower value of g^2 using the Schrödinger functional (SF) based scheme in agreement with its 3-loop step β -function [8], as shown in Fig. 4 (cyan color). In comparison, the dashed red line is the 3-loop

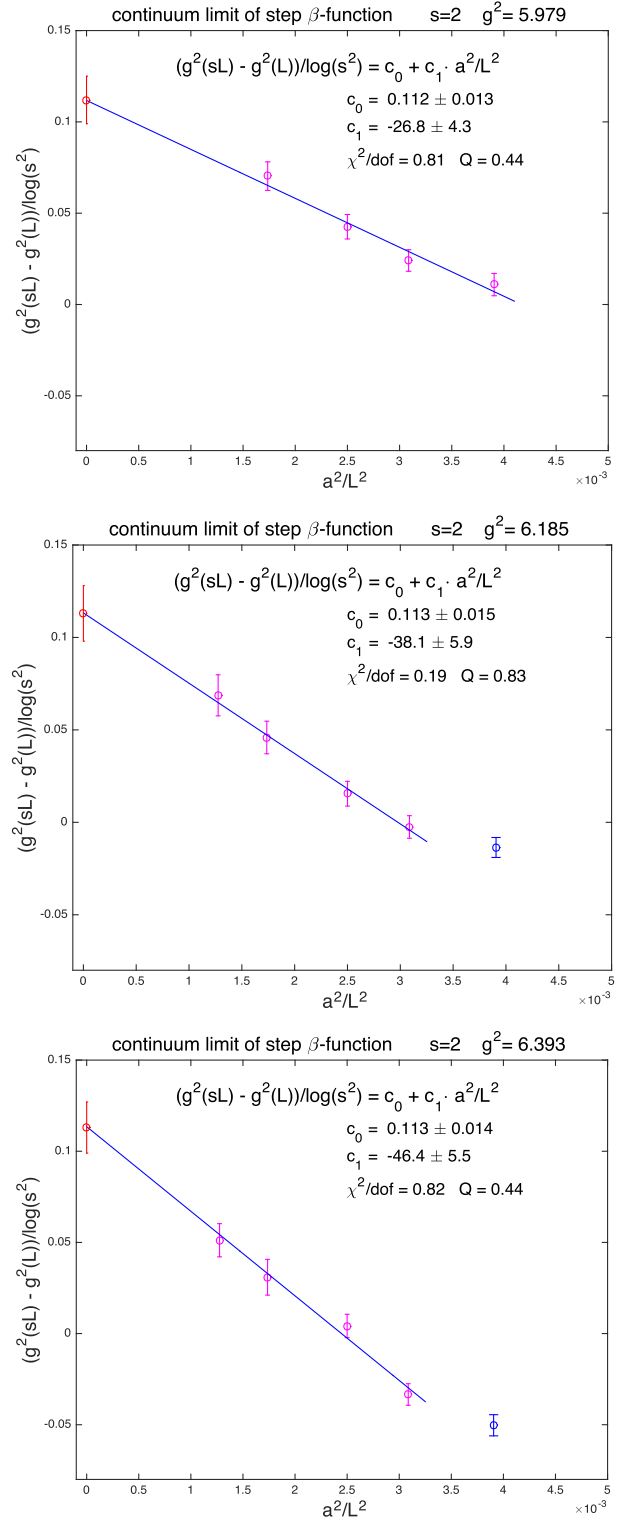


FIG. 3. Linear fits in a^2/L^2 are shown as explained in the text. The $16 \rightarrow 32$ steps of target B and target C are not included in the 4-point fits without any influence on the overwhelming statistical significance of the results. When they are included, the continuum step β -function drops lower by approximately one standard deviation with comparable errors and increased $\chi^2/\text{dof} \sim 1.5$, perhaps hinting at subleading small a^4/L^4 cutoff corrections at low L/a when the renormalized gauge coupling gets stronger.

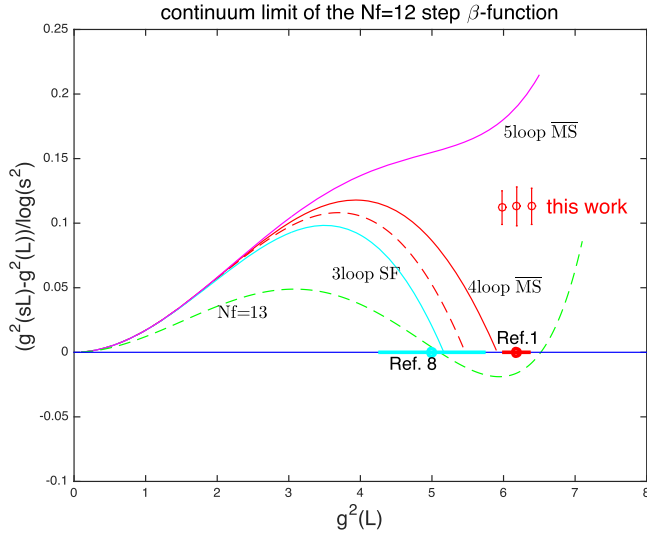


FIG. 4. The conformal fixed point of [6] and the three data points of our step β -function are shown (red color). The IRFP from [8] (cyan color) and the new 5-loop $\overline{\text{MS}}$ step β -function of thirteen flavors (dashed green) are discussed in the text.

prediction of the $\overline{\text{MS}}$ scheme within the simulation error of the IRFP. The 4-loop $\overline{\text{MS}}$ result only slightly shifts the prediction and is closer to [6]. Although in two different schemes, tantalizing agreement of the simulations and the loop expansion lead to the widely held view that twelve massless fermion flavors in QCD bring the theory inside the CW.

In a significant new development, the first $\overline{\text{MS}}$ calculation of the 5-loop β -function was completed for arbitrary flavor number in QCD [39]. Based on the new 5-loop results, it was immediately recognized that the zero in the β -function turns complex and the IRFP disappears for twelve flavors [40], consistent with the plot in Fig. 4. It was also shown that two fixed points appear in the β -function

for thirteen flavors like in the intriguing scenario of [41], with shifting estimates for the lower edge of the CW and for the flavor dependence of the mass anomalous dimension [40]. Five loop $\overline{\text{MS}}$ predicts two real zeros at $g^2 = 5.11$ and $g^2 = 6.52$ for thirteen flavors, as shown in Fig. 4. It did not escape our attention that new lattice studies of the running coupling with thirteen flavors would be within easy reach of the 5-loop $\overline{\text{MS}}$ predictions.

Credible proof of conformal behavior based on the β -function requires two necessary steps in strongly coupled gauge theories. First, the critical gauge coupling g_*^2 has to be determined where the scheme-dependent β -function vanishes and signals the location of the conformal IRFP. The slope of the β -function at the fixed point is a scheme-independent scaling exponent ω which controls the leading conformal scaling corrections to fermion mass deformations close to the IRFP [1,42–44]. The choice in scheme dependence can move the position of the conformal IRFP but cannot destroy its existence, or change the universal scaling exponent ω . These are very demanding criteria, unmatched in lattice simulations while reporting zeros in the β -function.

ACKNOWLEDGMENTS

We acknowledge support by the DOE under Grant No. DE-SC0009919, by the NSF under Grants No. 0970137 and No. 1318220, by OTKA under the Grant No. OTKA-NF-104034, and by the Deutsche Forschungsgemeinschaft Grant No. SFB-TR 55. Computational resources were provided by USQCD at Fermilab, by the University of Wuppertal, by Juelich Supercomputing Center on Juqueen, and by the Institute for Theoretical Physics, Eotvos University. We are grateful to Szabolcs Borsanyi for his code development for the BG/Q platform. We are also grateful to Sandor Katz and Kalman Szabo for their CUDA code development.

-
- [1] J. Kuti, Proceedings, *Proc. Sci. LATTICE2013* (2014) 004.
 - [2] Z. Fodor, K. Holland, J. Kuti, D. Negradi, and C. H. Wong, *Proc. Sci. LATTICE2013* (2014) 062.
 - [3] Y. Aoki *et al.* (LatKMI Collaboration), *Phys. Rev. D* **89**, 111502 (2014).
 - [4] T. Appelquist *et al.*, *Phys. Rev. D* **93**, 114514 (2016).
 - [5] T. A. Ryttov and R. Shrock, *Phys. Rev. D* **83**, 056011 (2011).
 - [6] A. Cheng, A. Hasenfratz, Y. Liu, G. Petropoulos, and D. Schaich, *J. High Energy Phys.* **05** (2014) 137.
 - [7] T. Appelquist, G. T. Fleming, and E. T. Neil, *Phys. Rev. Lett.* **100**, 171607 (2008); **102**, 149902(E) (2009).
 - [8] T. Appelquist, G. T. Fleming, and E. T. Neil, *Phys. Rev. D* **79**, 076010 (2009).
 - [9] R. C. Brower, A. Hasenfratz, C. Rebbi, E. Weinberg, and O. Witzel, *Phys. Rev. D* **93**, 075028 (2016).
 - [10] Z. Fodor, K. Holland, J. Kuti, D. Negradi, and C. H. Wong, *J. High Energy Phys.* **11** (2012) 007.
 - [11] Z. Fodor, K. Holland, J. Kuti, S. Mondal, D. Negradi, and C. H. Wong, *J. High Energy Phys.* **06** (2015) 019.
 - [12] Z. Fodor, K. Holland, J. Kuti, S. Mondal, D. Negradi, and C. H. Wong, *J. High Energy Phys.* **09** (2015) 039.
 - [13] Z. Fodor, K. Holland, J. Kuti, S. Mondal, D. Negradi, and C. H. Wong, [arXiv:1605.08750](https://arxiv.org/abs/1605.08750).
 - [14] G. Ferretti, *J. High Energy Phys.* **06** (2016) 107.

- [15] L. Vecchi, [arXiv:1506.00623](#).
- [16] T. Ma and G. Cacciapaglia, *J. High Energy Phys.* **03** (2016) 211.
- [17] C. Morningstar and M. J. Peardon, *Phys. Rev. D* **69**, 054501 (2004).
- [18] R. Narayanan and H. Neuberger, *J. High Energy Phys.* **03** (2006) 064.
- [19] M. Luscher, *Commun. Math. Phys.* **293**, 899 (2010).
- [20] M. Lüscher, *J. High Energy Phys.* **08** (2010) 071.
- [21] M. Luscher, *Proc. Sci. LATTICE2010* (2010) 015 [[arXiv:1009.5877](#)].
- [22] M. Luscher and P. Weisz, *J. High Energy Phys.* **02** (2011) 051.
- [23] R. Lohmayer and H. Neuberger, *Proc. Sci. LATTICE2011* (2011) 249 [[arXiv:1110.3522](#)].
- [24] Z. Fodor, K. Holland, J. Kuti, D. Nogradi, and C. H. Wong, *Proc. Sci. LATTICE2012* (2012) 050 [[arXiv:1211.3247](#)].
- [25] M. Luscher, *Nucl. Phys.* **B219**, 233 (1983).
- [26] P. van Baal, *Nucl. Phys.* **B264**, 548 (1986).
- [27] P. van Baal, *Nucl. Phys.* **B307**, 274 (1988); **B312**, 752(E) (1989).
- [28] A. Coste, A. Gonzalez-Arroyo, J. Jurkiewicz, and C. P. Korthals Altes, *Nucl. Phys.* **B262**, 67 (1985).
- [29] A. Coste, A. Gonzalez-Arroyo, C. P. Korthals Altes, B. Soderberg, and A. Tarancon, *Nucl. Phys.* **B287**, 569 (1987).
- [30] M. Luscher, P. Weisz, and U. Wolff, *Nucl. Phys.* **B359**, 221 (1991).
- [31] M. Luscher, R. Narayanan, P. Weisz, and U. Wolff, *Nucl. Phys.* **B384**, 168 (1992).
- [32] K. Symanzik, *Nucl. Phys.* **B226**, 187 (1983).
- [33] M. Luscher and P. Weisz, *Commun. Math. Phys.* **97**, 59 (1985); **98**, 433(E) (1985).
- [34] S. Duane, A. D. Kennedy, B. J. Pendleton, and D. Roweth, *Phys. Lett. B* **195**, 216 (1987).
- [35] J. C. Sexton and D. H. Weingarten, *Nucl. Phys.* **B380**, 665 (1992).
- [36] T. Takaishi and P. de Forcrand, *Phys. Rev. E* **73**, 036706 (2006).
- [37] U. Wolff (ALPHA Collaboration), *Comput. Phys. Commun.* **156**, 143 (2004); **176**, 383(E) (2007).
- [38] C. J. D. Lin, K. Ogawa, and A. Ramos, *J. High Energy Phys.* **12** (2015) 103.
- [39] P. A. Baikov, K. G. Chetyrkin, and J. H. Kühn, [arXiv:1606.08659](#).
- [40] T. A. Ryttov and R. Shrock, [arXiv:1607.06866](#).
- [41] D. B. Kaplan, J.-W. Lee, D. T. Son, and M. A. Stephanov, *Phys. Rev. D* **80**, 125005 (2009).
- [42] L. Del Debbio, B. Lucini, A. Patella, C. Pica, and A. Rago, *Phys. Rev. D* **82**, 014510 (2010).
- [43] L. Del Debbio and R. Zwicky, *Phys. Rev. D* **82**, 014502 (2010).
- [44] Z. Fodor, K. Holland, J. Kuti, D. Nogradi, C. Schroeder, and C. H. Wong, *Proc. Sci. LATTICE2012* (2012) 279 [[arXiv:1211.4238](#)].